

1000 High-redshift Galaxies with Spatially-resolved Spectroscopy: Angular Momentum over 10 Billion Years

Chris Harrison^{1,2}
Mark Swinbank²

¹ ESO

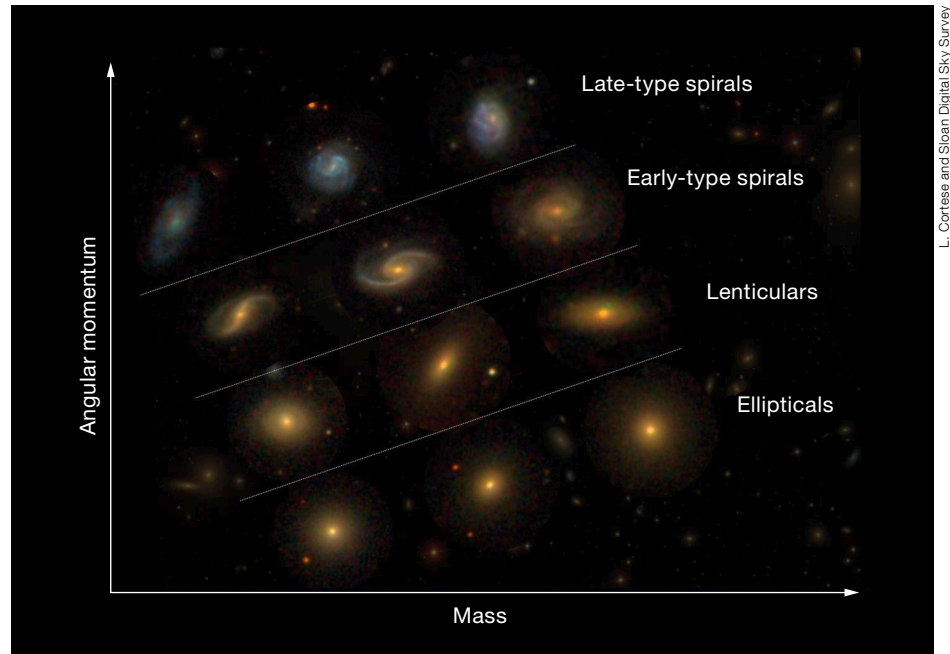
² Centre for Extragalactic Astronomy,
Durham University, United Kingdom

A sample of ~ 1000 high-redshift ($z \sim 0.3\text{--}1.7$) star-forming galaxies has been observed with three-dimensional spectroscopy using the KMOS and MUSE spectrographs in order to explore the dynamical properties of galaxies across cosmic time. A summary of the survey is presented along with one set of results that explores the relationship between the angular momentum of the star-forming gas and galaxy morphology. This work expands previous angular momentum studies that mostly focused on local galaxies, to cover the past 10 billion years of cosmic time.

Galaxy formation, morphologies and angular momentum

Galaxies have a range of morphological types, including ellipticals, spheroidals and late-type spirals, which form the morphological “Hubble Sequence”. Identifying the dominant physical processes that were responsible for the formation of the Hubble Sequence has been one of the major goals of galaxy formation studies for decades. In the cold dark matter paradigm, baryonic galaxies (i.e., the stars and gas) form at the centres of dark matter halos. If unperturbed, the baryons inside dark matter halos should cool and collapse, weakly conserve angular momentum and form a galaxy disc which follows an exponential light profile.

However, the angular momentum (i.e., the product of the mass, velocity and radial distance) of the baryons can also be redistributed through mergers, inflows, outflows and chaotic motions. From the dynamics of gas and stars of nearby galaxies, it has been shown that angular momentum appears to be the fundamental property defining the local Hubble Sequence (for example: Fall & Romanowsky, 2013; Cortese et al., 2016; see Figure 1). Indeed, Fall & Romanowsky (2013) show that local spiral discs retain $\sim 80\%$



of their initial angular momentum, but this drops to only $\sim 10\%$ for early-type ellipticals/spheroidals. As visualised in Figure 1, the Hubble Sequence of galaxy morphologies appears to follow a strict sequence of increasing angular momentum for a fixed mass.

The need for high-redshift integral field surveys

Morphological surveys of high-redshift galaxies, in particular using the Hubble Space Telescope (HST), have suggested that the Hubble Sequence began to emerge when the Universe was just under half of its present age (i.e., a redshift of $z \sim 1.5$; for example Mortlock et al., 2013). This is the epoch when spirals and ellipticals appear to become as common as irregular/clumpy galaxies. Consequently there is a clear need to expand local dynamical studies of angular momentum to galaxies in the distant, high-redshift Universe. Furthermore, recent simulations suggest that most of the angular momentum redistribution (that later defines galaxy morphologies) occurs at high redshift (for example, Lagos et al., 2017). If true, then the redistribution of angular momentum in high-redshift galaxies plays a dominant role in the formation the Hubble Sequence. Moreover, constraining the angular momentum of galaxies around

Figure 1. A schematic diagram showing the relative position of low-redshift galaxies with different morphologies in the angular momentum versus stellar mass plane.

this epoch (and any corresponding evolution) provides a critical test of galaxy formation models.

The most efficient way to obtain the required dynamical measurements for large samples of high-redshift galaxies is to use spatially-resolved spectroscopy, via integral field unit (IFU) data, to map bright emission lines such as $H\alpha$ or $[O\text{II}] 3727 \text{ \AA}$. Motivated by this, we set out to obtain measurements for almost 1000 galaxies out to $z \sim 1.7$, covering ~ 10 billion years of cosmic time, using two IFU instruments on the Very Large Telescope (VLT): the K-band Multi-Object Spectrograph (KMOS); and the Multi Unit Spectroscopic Explorer (MUSE).

Dynamics of 1000 high- z emission-line galaxies with KMOS and MUSE

For our studies, we constructed a sample of high-redshift ($z = 0.3\text{--}1.7$) star-forming galaxies with IFU data using two approaches: firstly, using KMOS Guaranteed Time Observations (GTO); and secondly, using archival MUSE observations. The KMOS spectrograph (Sharples et al.,

2013) has been in operation at the VLT since late 2012. KMOS has 24 near-infrared ($\sim 800\text{--}2500$ nm) IFUs that can be moved independently within a 7-arc-minute field of view. This enables the dynamics of large samples of high-redshift galaxies to be determined (at a rate that is $\sim 20\times$ faster than previously possible). The MUSE IFU (Bacon et al., 2010), which has been in operation since 2014, provides spectral coverage of the optical wavelengths, spanning $477\text{--}930$ nm and a contiguous field of view of 60 by 60 arcseconds. This combination of field of view and spectral coverage for an IFU means that large samples of high-redshift star-forming galaxies can be detected in emission lines — serendipitously — during any observation of an extragalactic field. Our results on the angular momentum of our combined MUSE and KMOS samples are presented across two papers — Harrison et al. (2017) and Swinbank et al. (2017) — and consist of data from the three observational surveys detailed below.

KMOS Redshift One Spectroscopic Survey (KROSS)

KROSS is a 30-night KMOS GTO project that was led by Durham University and the University of Oxford, with contributions from the University of Edinburgh (Stott

et al., 2016). The project ran from Period 92 to 95, and consists of a final sample of 743 star-forming galaxies at $z = 0.7\text{--}1.1$ (Harrison et al., 2017). All targets were observed in the YJ-band, targeting the $H\alpha$ emission line. The bright $H\alpha$ emission line enables us to map the two-dimensional gas dynamics on 3–10 kpc scales within these galaxies. Of the final sample, about 80 % are detected in $H\alpha$ emission, providing a sample of 586 galaxies for which dynamical measurements — and consequently angular momentum constraints — can be derived (Harrison et al., 2017).

KMOS Galaxy Evolution Survey (KGES)

KGES is an ongoing Durham University project utilising ~ 25 nights of GTO time on KMOS between Periods 95 and 100. Building on KROSS, the observations are designed to measure the dynamics of ~ 300 star-forming galaxies at $z = 1.3\text{--}1.7$. The first 17 galaxies from this survey are presented in Swinbank et al. (2017), and the results from the first half of the survey will be presented in Tiley et al. (2017).

MUSE serendipitous sources

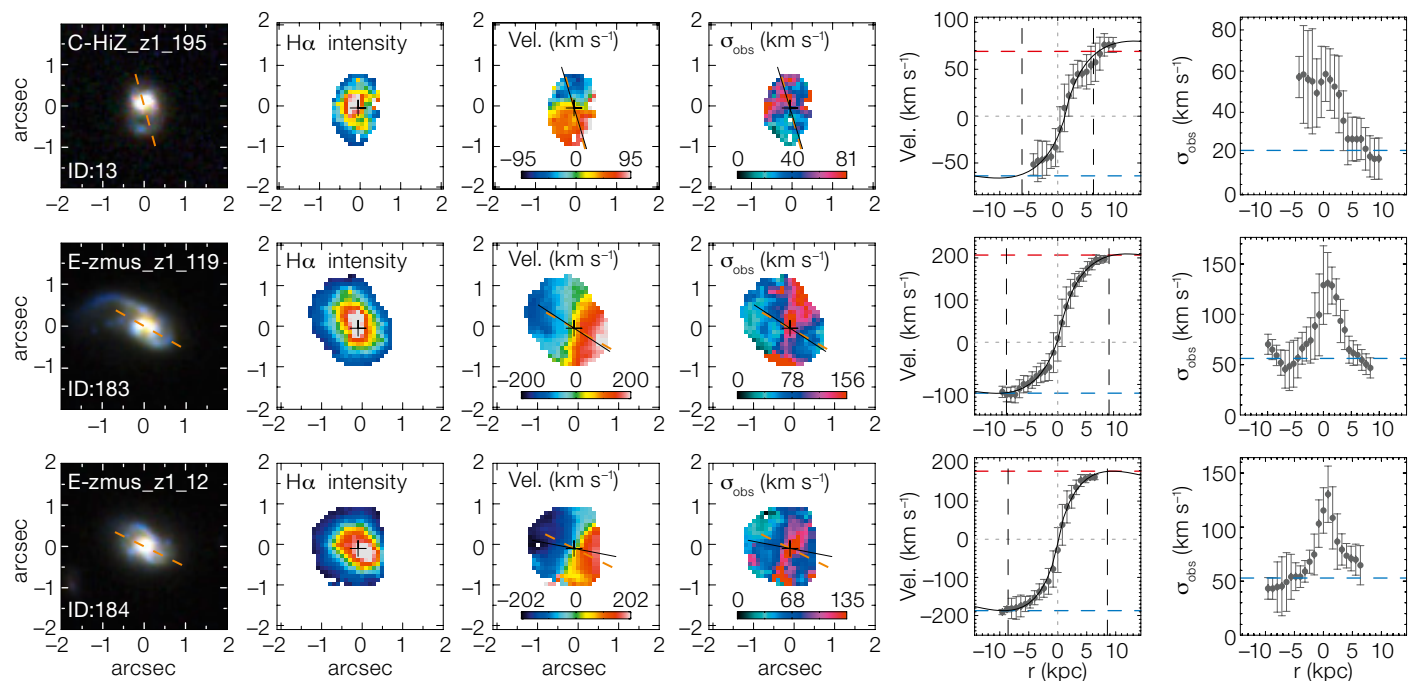
In order to extend the redshift and mass range of our KMOS survey, we exploited MUSE observations of 17 extragalactic “deep” fields that were observed during commissioning, Science Verification and Period 94. These fields include standard extragalactic “deep” fields (such as COSMOS), as well as high-redshift galaxies, quasars and cluster fields. By searching through the data cubes for the $[O\text{II}]$ 3727 Å emission line, we identified 364 star forming galaxies at $z = 0.3\text{--}1.7$ with sufficient data quality to perform dynamical analyses and consequently obtain angular momentum constraints (Swinbank et al., 2017).

Angular momentum of high-redshift star-forming galaxies

Using our KMOS and MUSE IFU data we produced maps of the emission-line gas intensity, velocities and velocity dispersions (i.e., random motions) for each galaxy. Examples can be seen in Figure 2. These maps were used to identify the

Figure 2. HST and KMOS data for three example objects. From left to right: (1) HST image (dashed line shows major axis); (2) $H\alpha$ intensity map; (3) velocity map; (4) velocity dispersion map (solid line shows

dynamical axis); (5) one-dimensional velocity profile (with model rotation curve overlaid); (6) one-dimensional dispersion velocity profile (with dashed lines showing intrinsic velocity dispersion).



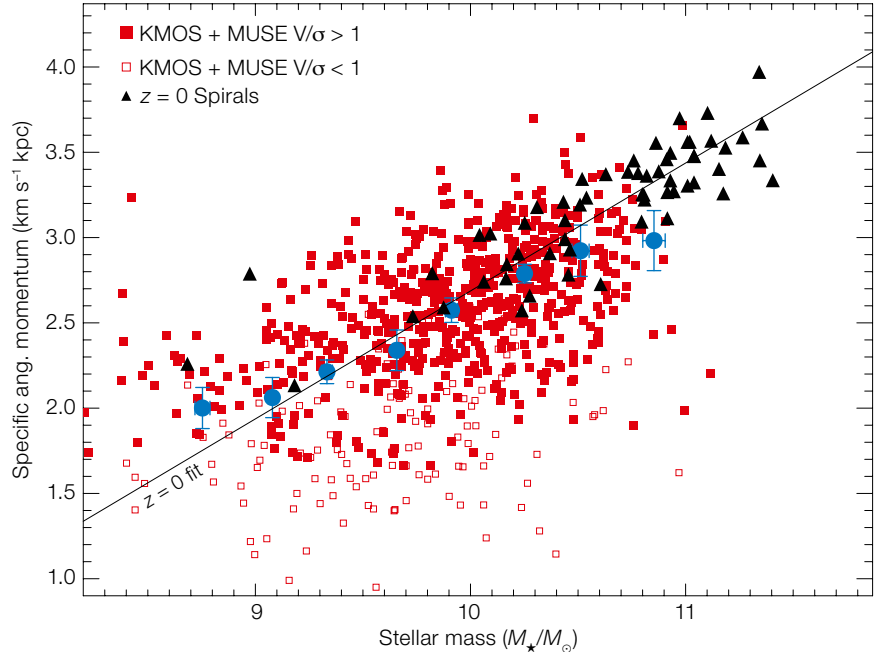
dynamical (“rotational”) axes of the gas and one-dimensional velocity profiles were extracted along these axes. Rotation velocities are measured at twice the half-light radii for each galaxy. The rotation velocity, in combination with the galaxy’s size, enables the angular momentum to be calculated. Throughout the analyses, great care was taken to remove any artificial “blurring” or “smearing” due to instrumental and atmospheric effects during the observations.

In Figure 3 we plot the specific angular momentum (i.e., the angular momentum per unit mass) as a function of the stellar mass for each galaxy in our sample. The relationship between angular momentum and galaxy mass for our high-redshift galaxies shows the same trend (i.e., slope) as seen in local galaxies (for example, Fall & Romanowsky, 2013). However, as discussed below, on average the high-redshift galaxies appear to have lower angular momentum than the spiral galaxies seen today (when the stellar masses are considered).

Angular momentum and morphology

By comparing the rotational velocities with the intrinsic velocity dispersions (see Figure 2), we determine whether the star-forming gas in each galaxy is predominantly “rotationally dominated”, or the galaxy is “dispersion dominated”. This is an important way to categorise the galaxies as it is strongly related to whether the galaxies are “discy” in nature. In Figure 3, the filled points show the galaxies that are dominated by rotation, versus those which are dominated by dispersion (open symbols). This shows that “discier” galaxies appear to have the most angular momentum. This is in qualitative agreement with the results sketched in Figure 1 for local galaxies — spiral galaxies have more angular momentum for a fixed mass than elliptical galaxies.

In order to test this result further, we isolated the galaxies with the most angular momentum per unit mass and those with the least angular momentum per unit mass and compared their HST images (see Figure 4 for examples). The galaxies with the highest angular momentum have the most prominent discs and spiral-like



morphologies. This may not be unexpected, but shows that the emergence of the Hubble Sequence in the high redshift Universe is closely related to the angular momentum of the star-forming gas. However, note that the discs in our high-redshift sample (see Figure 4) are not smooth, but consist of several “clumps” which may be the result of their relatively low angular momentum compared to their low redshift-counterparts (see below). In summary, the strong relationship between angular momentum, mass and morphology that is observed locally appears to be falling into place as early as redshift $z \sim 1.5$.

The evolution of angular momentum

The galaxies in our sample span a range of redshifts from $z \sim 0.3$ – 1.7 . To test how the specific angular momentum evolves with time, we split the sample into four redshift bins. However, to account for any underlying evolution of the stellar masses, we adopt the ratio of angular momentum of the stellar component to stellar mass ($j_*/M_*^{2/3}$), which should remove the expected underlying stellar mass evolution with redshift. In Figure 5 we plot this mass-normalised angular momentum as a function of redshift (and time). Also included on the plot are the locations of local galaxies of various morphological

Figure 3. Specific angular momentum (angular momentum per unit stellar mass; $j_* = J/M_*$) for the combined sample of high-redshift galaxies in the KMOS and MUSE samples. The high-redshift sample is split into those galaxies which are dominated by rotation (filled squares) and those that are dominated by dispersion support (open squares). Local spiral galaxies are shown as filled triangles. The run of the median specific angular momentum of the high-redshift galaxies is shown by the large blue points. The full KMOS + MUSE sample reveals a similar relationship between stellar mass and angular momentum as for local spirals.

types (early and late type spirals). Figure 5 reveals that selecting star-forming galaxies at increasing redshift (and time) results in selecting systems with decreasing angular momentum. To test how this compares to predictions from numerical models, we also include the evolution of angular momentum of model galaxies from the EAGLE¹ simulation (Schaye et al., 2015), selected in the same way as the galaxies in our observed sample. In both the data and the model, as star-forming galaxies increase their specific angular momentum, their morphologies transform into smooth spiral discs.

In summary, our results have shown that the fraction of rotationally supported disc-like galaxies at high-redshift is high, yet most of these galaxies appear clumpy (examples in Figure 4). We attribute the clumpy nature of the high-redshift galax-

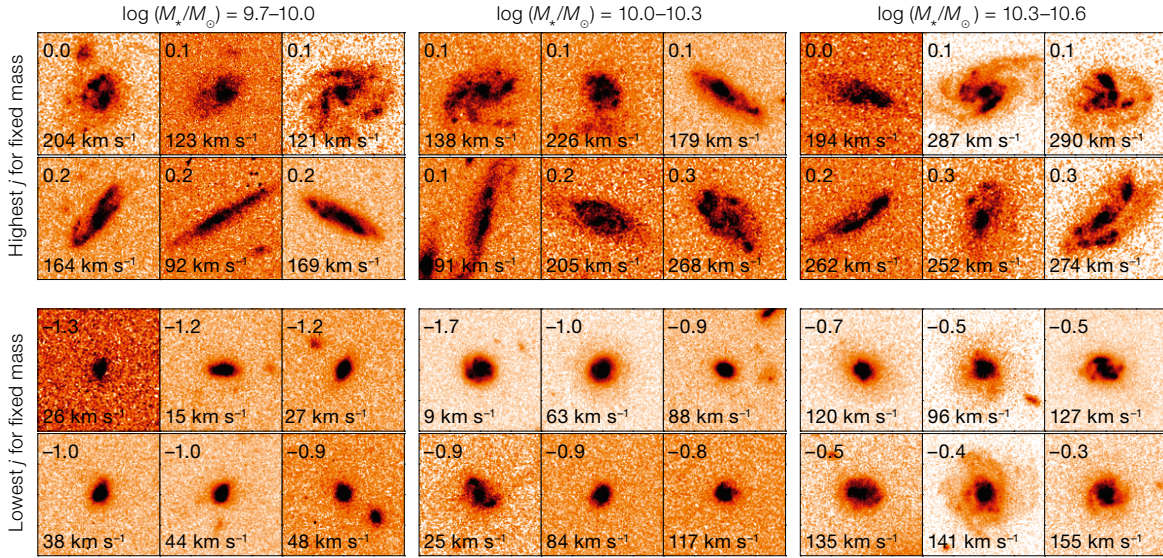


Figure 4. *I*-band HST images for the six galaxies from the sample with the lowest (lower panels) and highest (upper panels) specific angular momentum for three stellar mass bins. This shows that the galaxies with the highest angular momentum have the most prominent discs and spiral-like morphologies. The value in the lower left corner of each panel is the (inclination corrected) rotational velocity, and in the upper left, the value of $\Delta \log(j_i)$.

ies to the low angular momentum of the gas, which results in globally unstable, turbulent systems. With decreasing redshift, the angular momentum of gas discs appears to gradually increase (such as in Figure 5), and this appears to play a major role in defining the disc stability and morphology (Figure 4). As the specific angular momentum of growing discs increases below $z \sim 1$, the galaxy discs must evolve from globally unstable clumpy, turbulent systems into the stable, flat regular spirals we see today.

Ongoing work and prospects

The efficiency of KMOS and MUSE means that the next few years will see a continued increase in the sample sizes of galaxies with well resolved dynamics, but also in the range of stellar mass, star formation rate and redshift. In the near future, the launch of the James Webb Space Telescope will also allow the first systematic study of the stellar kinematics of high-redshift galaxies to be carried out, building on the work here which focuses on the star-forming gas kinematics. Confronting the gaseous and stellar content of galaxies will provide a critical measure of the interaction between star formation and gas dynamics, and further improve the constraints linking galaxy morphologies and angular momentum–mass–morphology relationships in galaxies around the peak epoch of galaxy formation at $z \sim 1.5$.

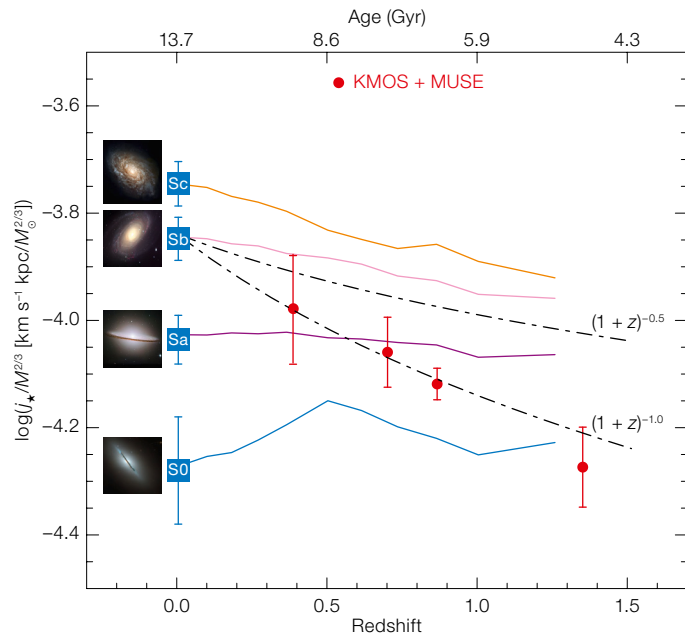


Figure 5. The redshift evolution of the specific angular momentum (normalised by mass) from $z = 0$ to $z = 1.5$. The $z = 0$ galaxies are split into their morphological types (from S0 to Sc). To compare with model predictions, the evolution of angular momentum for galaxies in the EAGLE simulation is overlaid. Toy-model tracks that show evolution according to $(1+z)^{-n}$ with $n = 0.5$ and $n = 1.0$ are also shown.

Acknowledgements

Based on observations data obtained under ESO programmes: 060.A-9100; 060.A-9302; 060.A-9306; 060.A-9318; 060.A-9321; 060.A-9323; 060.A-9325; 060.A-9326; 060.A-9331; 060.A-9334; 060.A-9338; 060.A-9460; 092.B-0538; 093.B-0106; 094.B-0061; 094.A-0141; 094.A-0280; 095.B-0035; 095.A-0570; 095.A-0748. The authors acknowledge support from the UK Science and Technology Facilities Council (ST/L00075X/1) and the Leverhulme Foundation.

References

Bacon, R. et al. 2010, SPIE Conf. Ser., 7735, 8
 Cortese, L. et al. 2016, MNRAS, 463, 170
 Fall, M. S. & Romanowsky, A. J. 2013, ApJ, 769, 26
 Harrison, C. M. et al. 2017, MNRAS, 467, 1965
 Lagos, C. d. P. et al. 2017, MNRAS, 464, 3850
 Mortlock, A. et al. 2013, MNRAS, 433, 1185
 Schaye, J. et al. 2015, MNRAS, 446, 521
 Sharples, R. et al. 2013, The Messenger, 151, 21
 Stott, J. P. et al. 2016, MNRAS, 457, 1888
 Swinbank, A. M. et al. 2017, MNRAS, 467, 3140

Links

¹ EAGLE Project: <http://icc.dur.ac.uk/Eagle/>